

D9 Bunched efficiency advanced study - 60 GHz

Final report on bunched efficiency

Task 9: Beam preparation

T. Lamy⁽¹⁾, L. Latrasse⁽¹⁾, T. Thuillier⁽¹⁾, M. Marie-Jeanne⁽¹⁾, C. Trophime⁽²⁾, F. Debray⁽²⁾, P. Sala⁽²⁾, J. Dumas⁽²⁾, C. Fourel⁽¹⁾, J. Giraud⁽¹⁾, I. V. Izotov⁽³⁾, A. V. Sidorov⁽³⁾, V. A. Skalyga⁽³⁾ and V. G. Zorin⁽³⁾

⁽¹⁾ Laboratoire de Physique Subatomique et de Cosmologie, Université Joseph Fourier Grenoble, CNRS/IN2P3, Institut National Polytechnique de Grenoble, 53 Avenue des Martyrs F-38026 Grenoble Cedex, France

⁽²⁾ Laboratoire National des Champs Magnétiques Intenses, CNRS, Université Joseph Fourier, 25 rue des Martyrs, 38042 Grenoble cedex 9, France

⁽³⁾ Institute of Applied Physics, Nizhny Novgorod, Russia

The beta beam project aims to use the β -decay of radioactive ions to produce neutrino beams. LPSC has proposed to develop a high frequency (60 GHz) pulsed ECR ion source prototype for beam preparation. In order to have efficient ionization, the ion source volume has to be small, and due to the ECR frequency value, the magnetic field has to be high (6 T at the injection, 3 T at the extraction, a closed surface with $|B| = 2.1$ T). The generation of the high magnetic field requires the use of helix techniques developed at LNCMI. As a first approach, a cusp structure has been chosen. 2D and 3D simulations were used to define the geometry of the helices. Calculus has shown that it is necessary to use two concentric radially cooled helices at the extraction side and two at the injection, using a pitch change for the internal injection coil. The results are above the initial specifications. An aluminum helix prototype of the internal injection coil has been used to validate at low current density the calculation of the magnetic structure. The electrical, mechanical and thermal characteristics are presented. A first version of the CAD mechanical design of the magnetic structure has been performed at LPSC and is under optimization to decrease the total volume of the source. The first 60 GHz magnetic structure (helices coils in their tanks, electrical and water cooling environment) is currently in fabrication for test measurements at half of the nominal current value, the measurement is scheduled for end of September 2009. An international collaboration has been setup and accepted by ISTC, it will permit the construction of the 60 GHz Gyrotron which is expected for the end of 2010.

Summary

1	<i>Context for the 60 GHz study</i>	3
1.1	The Beta-Beam project	3
1.2	Specifications for the pulsed ion source	3
1.2.1	High ion beam current	3
1.2.2	High radioactivity environment constraints	4
1.3	Discussion on the ECRIS capabilities	4
1.3.1	Advantages of the ECRIS	4
1.3.2	Challenges	4
2	<i>Preliminary study of the preglow mode at 18 and 28 GHz with PHOENIX-V2 and A-PHOENIX</i>	5
2.1	Experiment Description	5
2.2	Theoretical plasma model	7
2.3	Comparison of numerical and experimental results	8
2.3.1	Direct Comparison of Experimental and Simulated PGW Peaks	8
2.3.2	Gaussian Fit of the Experimental PGW and Parameters Simulation	9
2.4	Summary and strategy	10
3	<i>A 60 GHz Electron Cyclotron Resonance Ion Source for pulsed Radioactive Ion Beam production</i>	11
3.1	The 60 GHz Collaboration	11
3.2	The 60 GHz ECRIS magnetic structure	11
3.2.1	The resistive coils technologies	11
3.2.2	Design of a 60 GHz ion source in cusp configuration	12
3.2.3	60 GHz Magnetic CUSP specifications	13
3.2.4	Magnetic simulation	13
3.2.5	Validation with an aluminium prototype	15
3.3	Fabrication of the ECRIS prototype	16
3.3.1	Thermal calculations in helices	16
3.3.2	Engineering design	16
3.4	The future test bench	19
3.4.1	Bending Magnet for the 60 GHz bench	19
3.4.2	The 60 GHz Gyrotron	20
3.4.3	On-site installation for the half-magnetic field test	20
4	<i>Planning</i>	21
5	<i>References</i>	21
	<i>Related publications and communications</i>	22

1 Context for the 60 GHz study

1.1 The Beta-Beam project

The neutrino physicist community is currently discussing the next generation neutrino beam factory. Nowadays, several projects are still under competition. The Beta-Beam is a project studied by CERN. The baseline scenario is to generate, ionize, and then accelerate Radioactive Ion Beams (RIB) $\sim 5 \times 10^{13}/s$ ^{18}Ne or ^6He to high energies (with a Lorentz factor $\gamma > 100$). These nuclei which undergo β -decay are stored in a long race track decay ring to produce intense neutrino beams (see Figure 1 blue arrows). The goal of these beams is to study the neutrino oscillations properties and give constraints on the mixing angle θ_{13} .

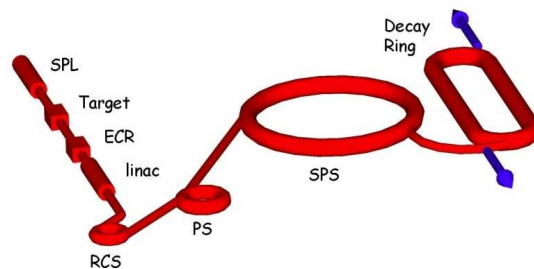


Figure 1. Baseline scenario of the beta-beam accelerator.

The radioactive elements are expected to be produced in the future EURISOL facility. The primary beam, delivered by a proton LINAC, induces nuclear reactions in a set of target stations. Radioactive gases effuse from the target to the ion source through a high conductance cooled pipe to filter gas and condensable contaminants. The ion source should bunch the beam in order to inject ions as efficiently as possible in the three synchrotrons rings included in the project.

1.2 Specifications for the pulsed ion source

1.2.1 High ion beam current

Consider an ideal source able to ionize the RIB of interest with 100% efficiency. If the ion extraction is performed in continuous working (CW) operation, the $5 \times 10^{13}/s$ ^{18}Ne flux would result in a 8 μA extracted CW beam. Such ionic intensity is very easy to extract from a classical Electron Cyclotron Resonance Ion Source (ECRIS). The Beta-Beam pulse width at the source extraction is expected to be $< 100 \mu\text{s}$, with a frequency repetition rate $f=1/T$ ranging within the 10 to 25 Hz range. The highest peak current, derived from these values is $\sim 8 \text{ pA}$. Moreover, other gases will be extracted from the target and ionized in the source. Thus, an unknown number of contaminants will be added to the extracted peak currents leading to higher total extracted currents. In such a situation, special attention should be taken for the extraction system, for example a multiple electrode with accel-decel configuration should be used, moreover the main high voltage supply should be carefully designed in order to avoid a too high voltage variation during the extraction of the pulsed beam.

1.2.2 High radioactivity environment constraints

The ^{18}Ne and ^6He half-lives ($T_{1/2}$) are respectively 1.67s and 0.807s. The time for a radioactive atom to exit the target and reach a classical ion source located several meters away already approximately reduces the initial atoms flux by a factor of 2. A key parameter for the project is to design an efficient ion source located as close as possible to the target in order to minimize the radioactive decay losses. Moreover, the source should hold radiation damages for a long time (~1 month). Consequently, the ion source mechanical parts can't contain permanent magnets or plastic gaskets; even radiation damage on glass fibre may cause problems. Due to the high radiation level, the maintenance of the ion source will not be possible and its cost per unit will have to be moderate, since it may be necessary to change it periodically.

1.3 Discussion on the ECRIS capabilities

1.3.1 Advantages of the ECRIS

ECRIS have shown high ionization efficiencies for noble gases (close to 100%).

Moreover, ECRIS can be used in continuous or pulsed operation. The pulsed operation, permitting to generate the well known afterglow mode (AFG) [1, 2], has been used daily at CERN for pulsed heavy ion beams production [3]. When varying the parameters (confinement magnetic field, microwave frequency and power, gas pressure, gas nature ...), different plasma regimes can be observed. The preglow mode (PGW) [4] takes place at the very beginning of the discharge when the microwave power is injected. The generation of 2×10^{13} ions of $^6\text{He}^{2+}$ or 8×10^{11} ions of $^{18}\text{Ne}^{6+}$, grouped in a 50 to 100 μs pulse, could possibly be achieved through the optimization of this process. Tests were undertaken within this design study for this purpose.

1.3.2 Challenges

1.3.2.1 Charge state distribution and RIB efficiency

However, due to the plasma processes involved in the device, a charge state distribution is extracted from the source, depending on the electronic configuration of the atoms to be multi-ionized and on the plasma characteristics. A physical limit of a RIB ion source efficiency comes from this 'natural' charge state distribution (CSD) generated by the plasma. In an ECRIS dedicated to the production of afterglow pulses, the hot electrons of the plasma along with a high magnetic confinement (τ_c) will favour high charge state ions extraction. The RIB of interest will then be extracted into several beams of different charge states. For example, in the case of neon, we can estimate that about 20 to 30% can be reached on one optimized average charge state (3+ to 6+) when 60 to 80% can be expected for an optimization on the 1+ charge. Nevertheless, it is still possible to design a special LINAC or a Fixed-field alternating-gradient accelerator (FFAG) to accelerate several charge states, i.e. two or three, at the same time. In this case, one can expect an increase of the overall maximum efficiency of the RIB ionization to reach ~30-50%. A second possible scenario is based on the studies initiated at IAP Nizhny Novgorod. There, a simple ECR magnetic trap (either axial mirror or axial CUSP) is used. Very powerful RF pulses (>100 kW) are used to build fast intense ions pulses. Recent promising results have shown the feasibility to produce very high currents up to 150 mA, and very short ions pulses (<100 μs) of low to medium charge states. We have tried to experimentally investigate the ionization efficiency, but due to a direct pumping in the

plasma chamber (which is not the case for classical ion sources) it has not been possible to get an evaluation of this efficiency. Another third possible scenario is to use a compact source with a low magnetic field to preferably produce low charge state ions. There, the ion charge state distribution follows naturally the Poisson statistics and the 1+ beam can be optimized to reach ~ 90% of the RIB of interest. Of course a special care must be taken to insure a high level of radioactive atoms ionization efficiency in the plasma.

1.3.2.2 Sources of losses for radioactive ions

One defines the residence time τ_r as the duration between the atom injection in the plasma chamber and its extraction through the plasma electrode hole, and τ_c as the confinement time of the plasma. A necessary condition to insure a negligible radioactive decay of the atoms in the source is to have $\tau_r \ll T_{1/2}$. If the plasma density is high, the ionization time will be very low and τ_r will be of the order of τ_c . Experimental confinement times in ECRIS are roughly in the range $\tau_c \sim 1-100$ ms, so $\tau_r \ll T_{1/2}$ is satisfied, provided the plasma to be dense. In pulsed mode, the radioactive atoms of interest can either be extracted as an ion beam, or as neutral gas. This last case will occur in case of too low plasma density. The plasma density of the ion source should definitely be as high as possible. Another cause of loss occurs if $\tau_c \ll T$ ($T=1/f$), f being the repetition rate of the HF microwave injection. In this case, the pulsed plasma disappears totally before the next pulse, letting room to natural gas diffusion through the electrode hole. When $\tau_c \sim T$, another source of loss comes from the low charge state afterglow extraction that will continue until the next RF pulse. These losses can be reduced by installing a pulsed valve at the gas injection, or by designing an iris able to close the electrode hole on trigger.

The plasma volume is also a critical parameter. We have seen that the foreseen pulsed RIB intensity to be extracted is high (>16 pA). Assuming the use of an innovative 60 GHz ECRIS with an electronic density near the cut-off $\sim 4 \times 10^{13}$ /cm³ and a plasma with an average charge $\langle Z \rangle$, the gas density necessary to insure the quasi neutrality condition (considering an ionization efficiency of 100%) will be $(4/\langle Z \rangle) \times 10^{16}$ atoms/liter, to be compared with the $\sim 5 \times 10^{13}$ /s RIB flux. If the plasma volume is large, the radioactive flux could be not sufficient to reach the high density plasma condition and a buffer gas flow will have to be added. The more the buffer gas flow, the higher the extracted pulsed beam intensity, and the higher the difficulties for the ion extraction. So the ion source should have a volume as small as possible in order to minimize the total extracted pulsed ionic current. A small volume is a challenging constraint for a 'standard model' complying ECRIS, since the use of superconducting technology requires a large volume to relax superconductor wire constraints.

2 Preliminary study of the preglow mode at 18 and 28 GHz with PHOENIX-V2 and A- PHOENIX

2.1 Experiment Description

The experiments have been performed on the PHOENIX-V2 ECRIS test bench described in details in [5]. The PHOENIX-V2 source is a modified version of the original PHOENIX one. The radial confinement magnetic field has been improved and the length of the hexapole reduced from 320 mm to 240 mm. The plasma chamber volume is ~ 0.7 liter. The minimum- $|B|$ structure of the ECRIS is obtained by the superposition of a radial hexapolar field ($B_r = 1.3$ Tesla at the plasma chamber walls) with an axial magnetic field forming a magnetic bottle

tunable within the following ranges: at the injection side the maximum magnetic induction is $B_{z\text{inj}} \leq 1.66$ T, in the middle plane $0.45 \text{ T} \leq B_{z\text{mid}} \leq 0.95$ T, and at the extraction side $B_{z\text{extr}} \leq 1.31$ T. The plasma is heated with a 28 GHz frequency microwave delivered by a Gycom gyrotron [6] with a 10 Hz repetition rate and a microwave pulse duration in the range of 5 to 15 ms. The total beam extracted from the ion source is analyzed through a 90° magnetic spectrometer and collected in a Faraday cup. The plasma electrode hole has a diameter of 10 mm and the extraction voltage is ranging from 30 to 40 kV. These values were chosen to get good beam transmission efficiency ($> 80\%$) throughout the 90° dipole to the analysis Faraday cup. The high transmission efficiency permits to consider that the ionic spectra obtained give a confident picture of the ECRIS plasma boundary conditions where the ions are extracted from.

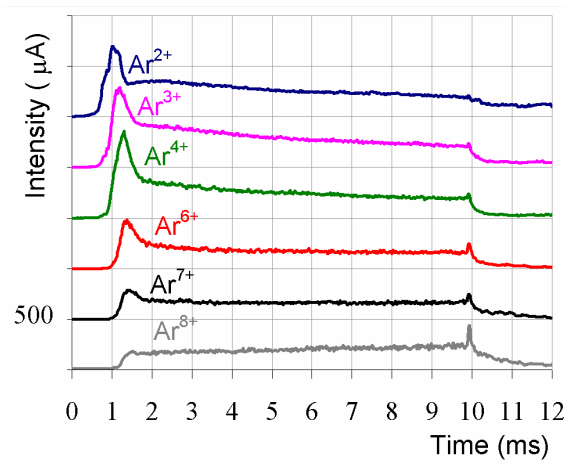


Figure 2. Example of experimental PGW peaks for argon. The microwave power is 3,1 kW, the extraction voltage is 30 kV, the pulse duration is 10 ms and the plasma electrode diameter is 10 mm.

The technique used to analyze the experimental ionic pulses is described in [7]. A typical time evolution of the multi-charged argon intensities for different charge states is presented on Figure 2, where the PGW peaks for charge states from 2+ to 8+ can be seen. The HF pulse begins at $t = 0$ and ends at $t = 10$ ms, the spectrum is optimized on the Ar^{4+} PGW peak due to a high gas flow used for the experiment. On the vertical scale the intensity between two sticks is $500 \mu\text{A}$, as the signals have been shifted up by this value for better view.

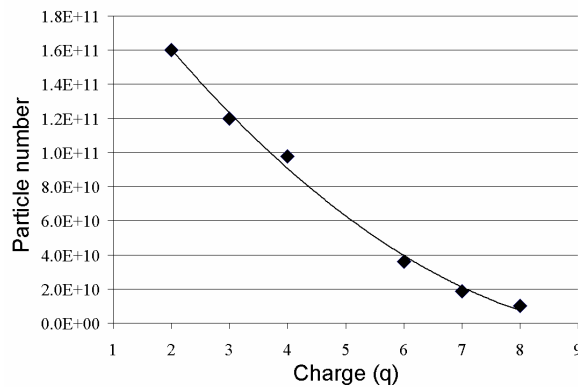


Figure 3. Number of ions in a $100 \mu\text{s}$ time window centred on the PGW peak maximum for each charge state.

The PGW peaks, whatever is the charge state, appear in the time range from ~ 1 to ~ 1.5 ms, this implies a fast ionization process with a hot and dense electron population. After 2 ms, the steady state is reached for every charge state, and at the end of the HF pulses (10 ms) the AFG peak increases for increasing charges. If we count the number of ions in a time window of 100 μ s centered on the PGW peak maximum for each charge state, we see that the maximum number is available on the Ar^{2+} , as shown in Figure 3.

2.2 Theoretical plasma model

In order to have a good understanding of the plasma characteristics evolution, a detailed analysis of the gas discharge ignition is necessary. The following description of PGW phenomenon is based on calculations which have been made with the zero-dimension plasma confinement model in a magnetic trap, which was firstly proposed in [8]. Significant additions to this model and calculations for different argon charge states have been performed and are presented in details in [9].

A microwave induced plasma ignition of a rarefied gas in a magnetic trap under the ECR conditions may be separated into two stages for which the growth rate of the plasma density is determined by different processes governed by the evolution of the electron energy distribution function (EEDF). At the first stage, the density is low and the electrons undergo a fast energy increase, the dominating process is the neutral gas ionization due to collisions with hot electrons. The plasma density at this stage grows fast, the gas ionization degree is low and the power absorbed by the plasma is less than the one absorbed at the steady state of the discharge. At the second stage, the increase of the density slows down significantly, the step by step ionization process goes further modifying the EEDF, the average charge state increases, and the power absorbed by the plasma is approximately equal to the value at the steady state.

The initial stage of the plasma ignition, when the density is sufficiently low, can be described with the theory for a microwave breakdown of a rarefied gas in axi-symmetric mirror magnetic traps under the electron cyclotron resonance conditions [10]. In this work, an important factor which significantly affects the EEDF shape is the superadiabaticity effect. When the plasma density is so low that the electron collision time is much longer than the interaction time of an electron with the HF wave in the resonance region, the energy transfer can be described like for a single electron. The ECR energy increase of the lone electron in a mirror trap is governed by stochasticity, and this remains true when the phase change of the microwave between two electron passes through the ECR zone is much more than 2π [10]. With the electron energy increase, the electron travel time from mirror to mirror decreases and consequently the phase variation of the heating wave decreases too, this means that at a certain electron energy value the stochastic mechanism of electron heating is destructed. At this stage the interaction of hot electrons with a microwave is called superadiabatic interaction. The consequence of this interaction is an electron energy limitation which is called superadiabaticity effect. Hence, while the plasma density is low, the plasma is unable to absorb more energy than a certain value, because the energy of every electron is limited. An example of such a superadiabatic EEDF at the very beginning of an ECR discharge is plotted in Figure 4.

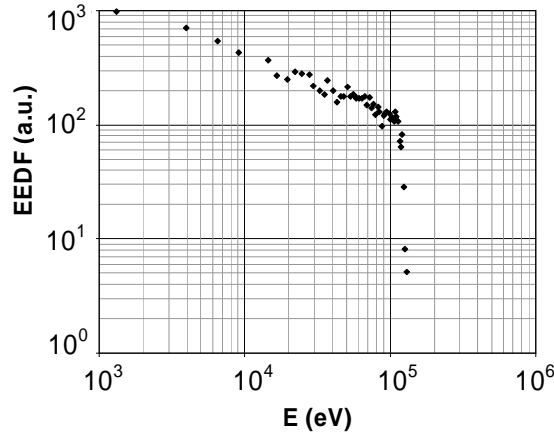


Figure 4. Example of a superadiabatic EEDF.

When the plasma density increases further, the absorbed heating power becomes insufficient to maintain the EEDF. This happens when the total energy, absorbed since the beginning of the discharge, equals to the sum of the energy lost in the plasma leaks from the trap and in the ionization processes.

2.3 Comparison of numerical and experimental results

2.3.1 Direct Comparison of Experimental and Simulated PGW Peaks

The previous described model has been used in order to simulate experimental argon PGW peaks shown on Figure 2. The time evolution of the ionic currents has been computed simultaneously for all argon charge states with a predefined set of free parameters. For each argon charge state, the corresponding numerical fit was calculated; the experimental measurements with the corresponding fit are shown in Figure 5 for Ar^{3+} and Ar^{4+} and Ar^{6+} . The best fit has been obtained with the free parameters set as follows: absorption rate = 25 % and upper limit for transversal lifetime = 600 μs . There is a good agreement between numerical simulations and experimental data for charges lower than 4+ where the PGW peak intensity is well reproduced. However these peak intensity values are overestimated for higher charges, it can be explained by the approximate calculation of the transversal ion lifetime which strongly depends on the ion charge states. In Figure 5b) we have plotted the calculated electron energy averaged over the EEDF, after about 1ms due to the transition between the superadiabatic EEDF and the Maxwellian one, the average electron energy begins to collapse.

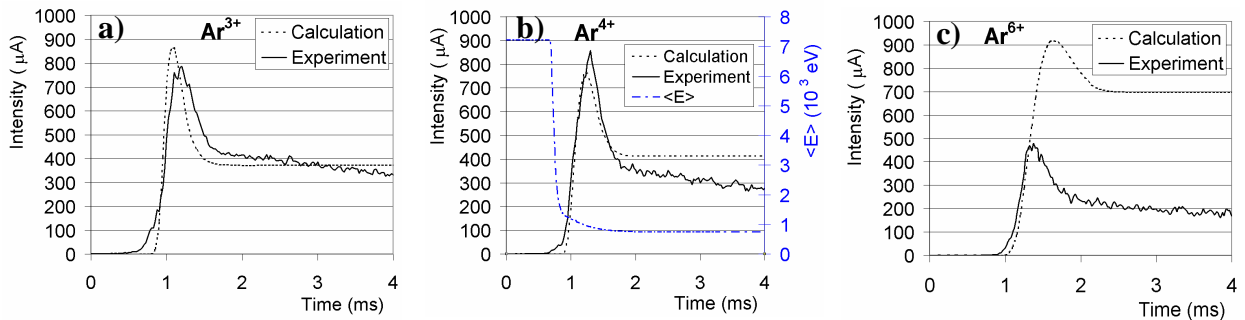


Figure 5. Experimental Ar pulses and their numerical fits for a) Ar^{3+} , b) Ar^{4+} and calculated $\langle E \rangle$, c) Ar^{6+} .

2.3.2 Gaussian Fit of the Experimental PGW and Parameters Simulation

In order to study the PGW peak characteristics, several parameters have been introduced for convenience based on the results of a Gaussian fit of the PGW peaks. The PGW parameters, presented in

Figure 6, are as follows: I_{max} is the peak maximum current, FWHM is the peak full width at half-maximum, $T_{I_{max}}$ is the time to reach the maximum intensity ($t=0$ being microwave trigger) and T_{10} is the time to reach 10 % of I_{max} . The PGW peak is not symmetric, so the fits were made using mainly the left part of the curve, i.e. for time $t \leq T_{I_{max}}$.

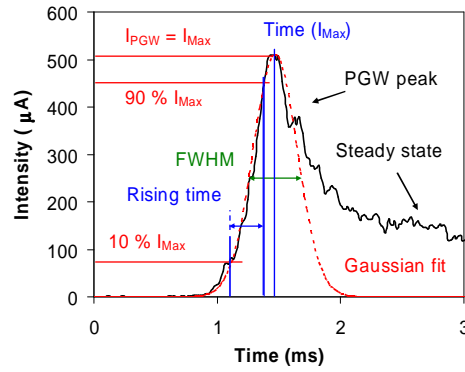


Figure 6. Experimental PGW along with a Gaussian fit.

The variations of such PGW parameters as T_{10} , $T_{I_{max}}$, FWHM and I_{max} with the ion charge states are shown Figure 7, in the case of the experimental conditions described in the section 2.1 (microwave power = 3100W). To check the validity of the simulation of the peak intensities, the microwave power has been varied; these results are presented in [9].

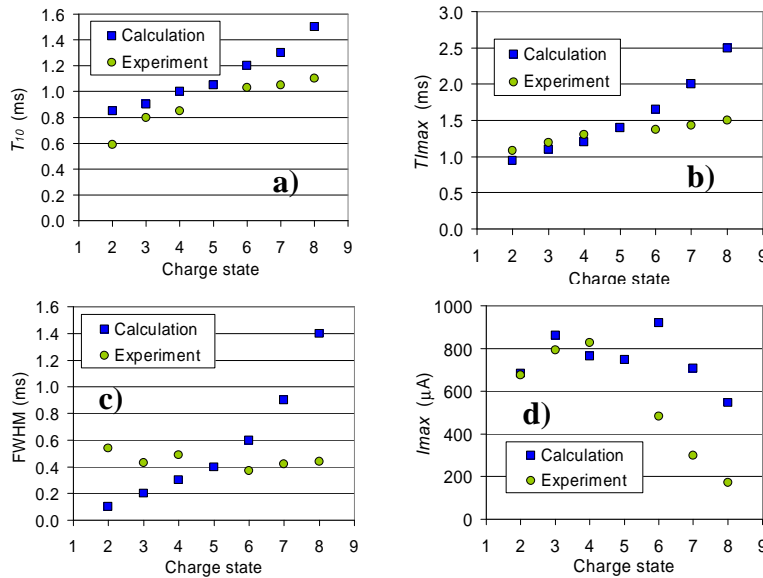


Figure 7. Preglow peaks characteristics for a microwave power of 3100 W ($P=16W/cm^2$): comparison between experimental and numerical fits for a) T_{10} b) $T_{I_{max}}$ c) FWHM d) I_{max} .

It is visible on Figure 7 that the proposed numerical model is able to predict the main PGW parameters dependences for charge states $q = 2, 3$ and 4. A huge deviation appears for higher charge states, not due to charge exchange processes which were included in the simulation. The evolution of the I_{max} values obtained by the simulations for the consecutive charge states

presents one or two maxima: they could be due to competitive effects that have not been yet identified by the authors. The general agreement between calculations and experimental results allows us to propose an explanation of the PGW phenomenon based on the results of the computer modeling. In Figure 5c) the Ar^{4+} PGW peak is presented together with the calculation of the average electron energy in the discharge. After $t \approx 1$ ms, the fall away of $\langle E \rangle$ is connected with the plasma density overrunning the level where the EEDF transits from superadiabatic to Maxwellian. Further plasma density increase leads to a decrease of $\langle E \rangle$. The longitudinal lifetime is decreasing as a result of the $\langle E \rangle$ dropping which provides a fast plasma outlet from the ECRIS and the formation of a PGW peak.

The only experimental parameter we could not change during experiments was the microwave frequency, the PHOENIX-V2 ion source having only one microwave injection port. The relatively good agreement between experimental results and simulations, in the case of Ar^{4+} , allows us to make a qualitative numerical estimation of the evolution of the PGW parameters with the microwave frequency. In this simulation, other parameters of modeling were chosen to maintain the same charge state distribution along the microwave frequency scale. It is visible on Figure 8 that the PGW intensity is increasing and the time width of the signal is decreasing for higher microwave frequencies. The use of frequencies higher than 28 GHz associated with higher microwave power injection will permit to increase the plasma density and then should permit to increase PGW efficiency for high charge states.

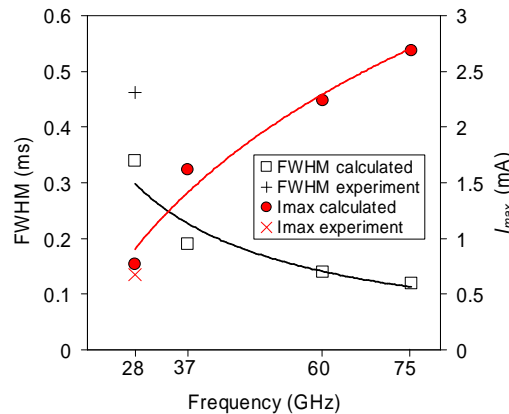


Figure 8. Microwave frequency influence on PGW parameters

2.4 Summary and strategy

To produce neutrino beams, the use of intense and pulsed accelerated radioactive ion beams is under evaluation for the Beta Beam project connected to the EURISOL facility. When using radioactive ion beams, efficiency is an important parameter. The work presented here does not evaluate nor measure the efficiency, however it shows the possibility to produce intense pulsed beams about one order of magnitude below the expected intensities for the beta beam project and shows a potential increase of this intensity when using higher microwave frequencies. The authors expect that future study of the Preglow phenomenon under conditions of 60 GHz microwave ECR heating should effectively show the Preglow peak FWHM reduction, and an intensity increase leading to the expected intensity level.

The Beta Beam Pulsed Ion Source high plasma density implies high current extraction. A 4th generation ECRIS, with RF > 50GHz, seems to be the best option. The volume should be as small as possible in order to limit the total extracted current. In order to investigate the

topic, the LPSC team decided to start an ambitious 60 GHz R&D program. The goal is to build several prototypes of 60 GHz innovative magnetic structures and test them in pulsed mode.

3 A 60 GHz Electron Cyclotron Resonance Ion Source for pulsed Radioactive Ion Beam production

3.1 The 60 GHz Collaboration

The project brings together many partners with versatile skills. Thus, three partners collaborate in order to build a test bench dedicated to the study of the bunching efficiency at 60 GHz:

- The Laboratoire de Physique Subatomique et de Cosmologie (LPSC), based at Grenoble in France, is a specialist in ECRIS and low energy beam line. It is the main actor of this project, in charge of the design and fabrication of the ECRIS with its test infrastructure.

- The Laboratoire National des Champs Magnétiques Intenses (LNCMI), based in Grenoble, is a specialist of very high magnetic fields, particularly in resistive coils technology. LPSC has taken profit of LNCMI experience in high magnetic fields to build an innovative ion source magnetic structure.

- The Institute of Applied Physics (IAP), in Nijni Novgorod in Russia, is a specialist in plasma physics, gyrotrons and pulsed ECRIS. Their task is to improve the theoretical tools to simulate real experiments, and provide the 60 GHz gyrotron.

3.2 The 60 GHz ECRIS magnetic structure

3.2.1 The resistive coils technologies

For the construction of the high magnetic field, we collaborate with LNCMI in Grenoble who uses two main technologies, the Bitter and the polyhelix technique. The elementary part of a Bitter magnet shown in Figure 9 is a plate of highly pure copper in which the electrical current flows. The plates are stacked and pressed together with intermediate thin insulating layers of polyimide (eg. Kapton). In this manner each plate (or plates in parallel) forms a turn of the winding. Preliminary calculations have shown that it was possible to produce a mirror field with two maxima of 4 and 7 Teslas distant of 200 mm with 3 coils. The other technique is the helices technology: the coil helices are made of copper alloy cylinders into which a helical slit is cut by electro erosion. The current density can be more important in this latter technology. Figure 9 shows a polyhelix assembly of 14 concentric coils.

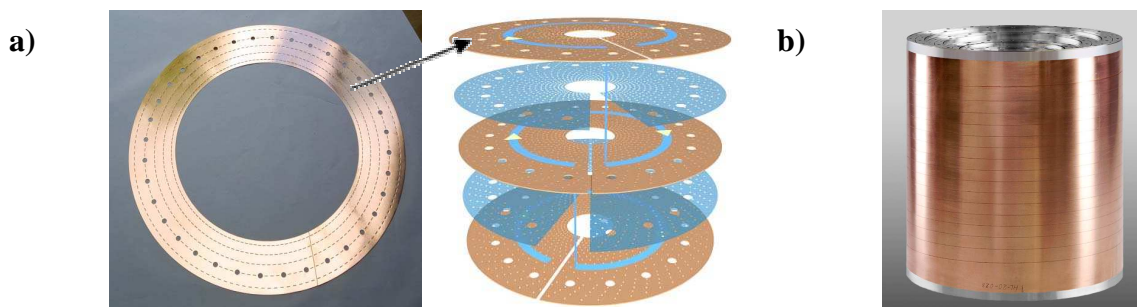


Figure 9. (a) Bitter disk and Bitter assembly. The inner diameter is 400 mm. (b) polyhelix assembly.

The 60 GHz prototype will take benefits of the advantages of these high field techniques in term of:

- Compacity: thanks to the high heat transfer coefficient obtained it is possible to enhance the current density up to 30 000 A/cm² in Bitter coils and 60 000 A/cm² in radially cooled helices.
- Versatility: contrary to classical impregnated coils, the techniques allow a step by step development as it is possible to adapt locally the coil current density by changing the thickness of the plates in the Bitter case or the helix pitch along the copper coil in the polyhelix case.

The first magnetic structure chosen to be developed is a cusp with a closed resonance zone, the technology chosen for this CUSP is the polyhelix technology, however Bitter coils should be used with or without polyhelix technology for other magnetic configurations.

3.2.2 Design of a 60 GHz ion source in cusp configuration

The structure foreseen may be as simple as a single field gradient to a complex minimum-|B| structure. The development of several operational superconducting technologies at 60 GHz permitting R&D studies is not realistic since it takes a lot of time and requires a lot of money. The collaboration with the LNCMI allows making easily 60 GHz ECRIS R&D for an affordable price, a reduced design time and the minimization of risk the technology being classical (copper and water). LNCMI is equipped with a set of 20 MW/35 Tesla resistive coils available for fundamental physics studies. The original idea consists in developing 60 GHz prototype magnetic coils using the helix coil resistive technology [12] invented at LNCMI and test them on site, with a new dedicated ECRIS test bench. The 60 GHz prototypes will be dimensioned to comply with the LNCMI electrical power and water cooling systems. Moreover, this technology is usable in a highly radioactive environment, since the magnetic structure is mainly composed of copper, steel and water.

The 60 GHz prototype will be built in several steps: a first prototype consists in a simple axial mirror trap when the second one will have a radial confinement. It has been shown before, that a small volume ion source with an efficient magnetic confinement was desirable to reach high efficiencies. Due to the high extracted currents expected, a specific effort should be performed on the extraction system.

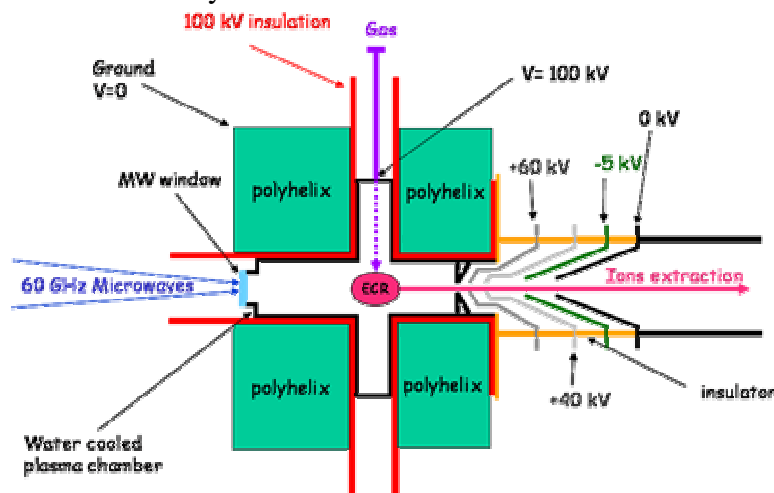


Figure 10. Sketch of the 60 GHz first prototype ECR ion source in cusp configuration.

The Figure 10 represents a sketch of the 60 GHz first prototype ECR source in cusp configuration. The water cooled plasma chamber has a shoulder to have a good magnetic mirror. Two sets of coils are necessary to produce the magnetic configuration expected. The plasma chamber may be put at a voltage of 100 kV and is isolated from the other parts of the installation. Microwaves are injected on the injection side while the gas is injected by the shoulder. A multi-electrode system will permit the extraction of the beam.

3.2.3 60 GHz Magnetic CUSP specifications

As a first step, LPSC and LNCMI decided to design an axi-symmetric MHD stable magnetic structure: a cusp. The initial design specifications include the following magnetic properties (see Figure 11): a closed 2.1 Tesla 60 GHz ECR zone, a 4 Tesla radial mirror; a 6 Tesla axial magnetic field at the injection; a 3 Tesla axial magnetic field at the extraction, a 100 mm mirror length. Field lines going through the ECR zone must be connected to the magnetic mirrors without intercepting the plasma chamber wall.

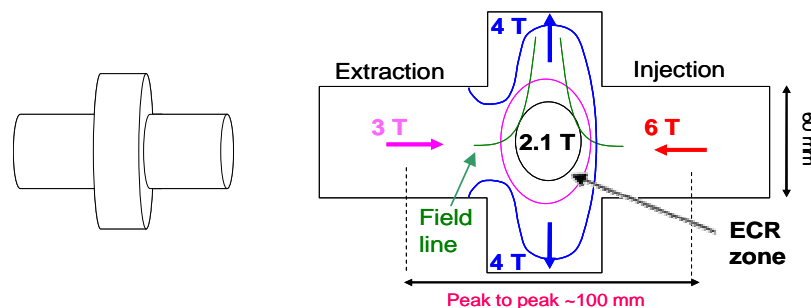


Figure 11. Magnetic field expected in the plasma chamber.

3.2.4 Magnetic simulation

A 2 dimension (2D) simulation was first performed using both RADIA [13] and Getdp (developed at Liege University) codes, specially adapted to the helix technique [14]. A flexible solution has been found with a set of 4 radially cooled helices coils, named H1, H2, H3 and H4, visible on Figure 12:

- H1, the longest helix, mainly generates the magnetic field at injection. H1 is composed of three successive pitch areas. The shortest pitch is located on the inner side of the source, close to the largest diameter of the plasma chamber (shoulder), to concentrate the closed ECR zone and generate radial mirror.
- H2 is very short and permits to keep the ECR zone close to the centre of the source and to generate the radial mirror.
- H3 and H4 help to generate the radial mirror in the shoulder.
- H4 mainly produces the extraction magnetic field.

The concentration of a high magnetic field gradient in a 100 mm peak to peak axial cusp rendered the optimization difficult. When the distance between the injection and extraction coils is small, the radial magnetic mirror value is high (sum of radial magnetic components), but consequently the axial magnetic peaks at injection and extraction are reduced (subtraction of the axial magnetic component). A compromise was found when the smaller inner radius of the coils was close to the distance between them. The inner plasma chamber diameter was set to the minimum value possible (60 mm). The corresponding inner coils diameter was set to 80

mm. Below this diameter, the condition stating that the field lines should not cross the walls of the plasma chamber could not be fulfilled.

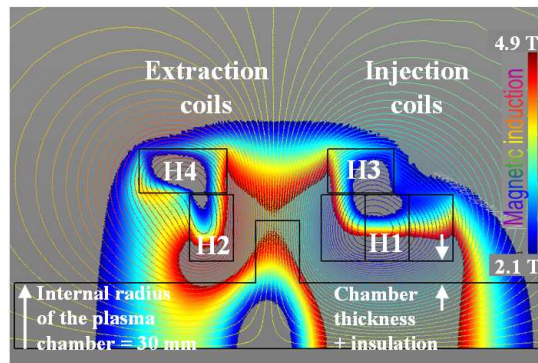


Figure 12. 2D simulation with pitch change configuration of H1. Half of the plasma chamber is represented.

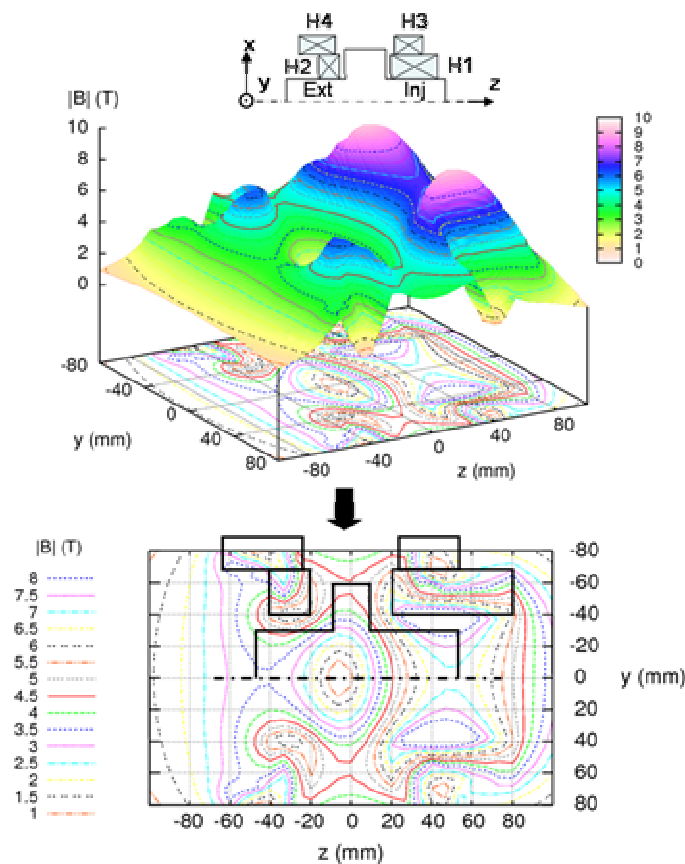


Figure 13. 3D simulation and projection of the magnetic field $|B|$ in the $Oy-Oz$ plane.

The simulation continued with 3D calculations done with another code still based on Getdp [15]. It includes thermal analysis (helices water cooling) and exact helices geometry (width of the electro erosion slit) which was not the case in the 2D calculation. The helices were designed with CATIA and then meshed by SAMCEF Field. The current injected in the coils is 30000 A. The conductivity of the helices is 90 % of the International Annealed Copper Standard (IACS). 3D simulation gave results in good agreements with the 2D ones. Figure 13, represents the magnetic field norm $|B|$ in the $Oy-Oz$ plane as calculated with the 3D

simulation. The magnetic field intensity reaches 6.9 T at the injection on the z axis and 3.4 T at the extraction. The radial mirror intensity varies between 4.8 and 4.9 T, due to the imperfect helices symmetry. The magnetic structure can be seen in 3 dimensions using the EnSight 8 software. Thus, in Figure 14(a), the components of the magnetic field are represented in the plasma chamber. The Figure 14(b) represents the norm of the magnetic field in the plasma chamber and the temperature in the helices. Note that the temperature calculated in this simulation does not take into account the insulator areas between the turns of the coil to maintain the space between the turns and prevent short-circuit (see section 3.3.1). These values of the magnetic field are above specifications, so more tuning flexibility will be available for the ion source.

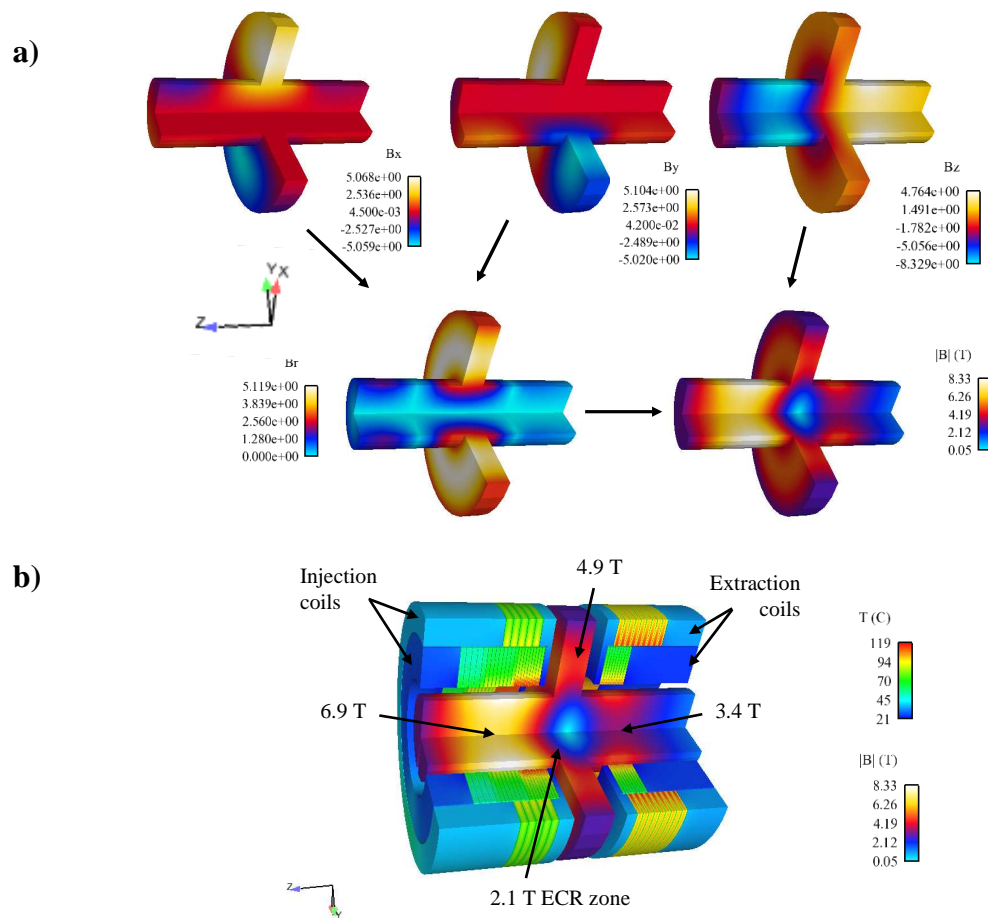


Figure 14. (a) Component of the magnetic field in the plasma chamber. (b) Norm of the magnetic field in the plasma chamber and temperature in the helices.

3.2.5 Validation with an aluminium prototype

Since the design includes an innovative small pitch of 2 mm (winding thickness = 1.7 mm, space between 2 windings = 0.3 mm) never used before, an H1 aluminum helix prototype has been machined at scale one to experimentally test the accuracy of the calculations (see Figure 15(a)). Figure 15(b) represents a comparison between the calculated axial magnetic field and the measured axial magnetic field along the coil axis at low current density (144 A injected). $z = 0$ mm is the beginning of the helix on the thin pitch side. The difference is only of 3 % at the maximum peak value and both curves have the same magnetic center. The test validates

the simulation and allows to start building the magnetic structure.

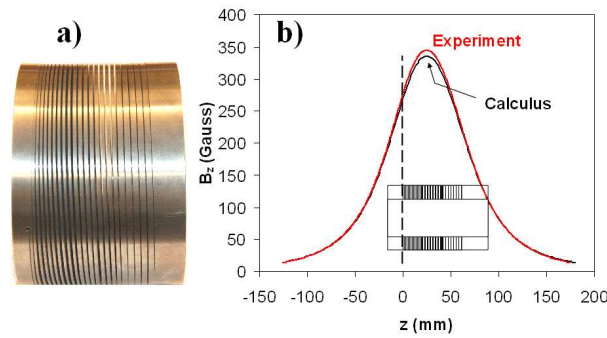


Figure 15. (a) H1 aluminum prototype, (b) Axial magnetic profile of H1.

3.3 Fabrication of the ECRIS prototype

3.3.1 Thermal calculations in helices

To maintain the space between the windings and have a constant pitch and to prevent short-circuits, it is mandatory to insert insulator areas between the windings of the coil. Typically, 20 to 24 insulator areas are necessary to support the repel forces generated by the magnetic field and avoid the contact of 2 windings between two insulator areas. The total surface of the insulator represents around 10 % of the surface of a winding. The Figure 16 represents a part of a winding of the less thick pitch, i.e 2 mm (corresponding to a winding thickness of 1.7 mm), of the internal injection coil H1. 12 insulators areas are distributed on the whole winding. The heat transfer is $79000 \text{ W/m}^2/\text{°C}$ and there is no cooling considered under the insulators. The cooling flux $Q = 24 \text{ L/s}$ and the intensity $I = 24000 \text{ A}$. Calculus show that at full current, the mean temperature should reach 180 °C ($I = 30000 \text{ A}$, $Q = 29 \text{ L/s}$, $h = 84000 \text{ W/m}^2/\text{°C}$ and a winding thickness of 1.7 mm), and that the maximum temperature should not exceed 330 °C .

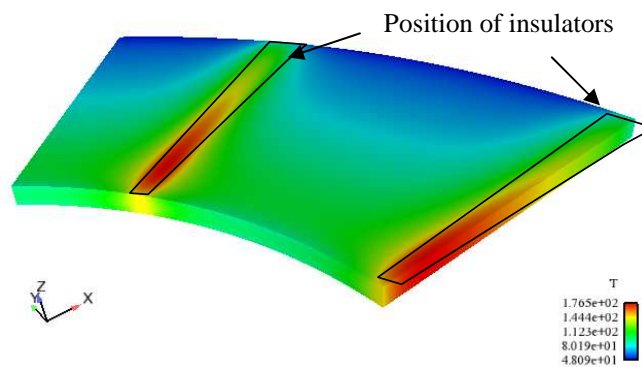


Figure 16. Thermal calculation in a part of a winding. Winding thickness = 1.7 mm, intensity $I = 24000 \text{ A}$, cooling flux $Q = 24 \text{ L/s}$, heat transfer $h = 79000 \text{ W/m}^2/\text{°C}$.

3.3.2 Engineering design

3.3.2.1 Electrical and cooling needs

The current intensity in the cusp has been chosen to be 30000 A. Calculations have been performed using a conductivity of 86.5 % IACS. Thus, the maximum current density reaches 640 A/mm^2 on the internal radius of H1 and H2, where the pitch is only of 2 mm. The electrical power needed is about 6 MW, depending on the final coils resistivity, so the structure is actively cooled by de-ionized water. The inlet water pressure is 2.7 MPa (27 bars), while the outlet one is 0.4 MPa (4 bars). The average water temperature increase is 20°C . The water flow rate is 24 to 29 l/s in the two set of coils. The water speed in the radial helices slit ranges within 16 to 35 m/s, providing a convection heat transfer coefficient $h \sim 80$ to $160 \text{ kW/m}^2/^\circ\text{C}$, depending of the coil. The average coils temperature varies from 80 to 180°C while the peak temperature locally reaches 330°C .

3.3.2.2 CAD Design and Mechanical Calculus

Rings are mandatory to allow the passage of the current from internal to external coils. Nevertheless, in order to minimize the distance between injection and extraction coils (to favor the magnetic mirror field), the rings are integrated to internal coils, as shown in Figure 17. The integrated rings possess recesses on internal coils and keys on external coils to support the radial forces.

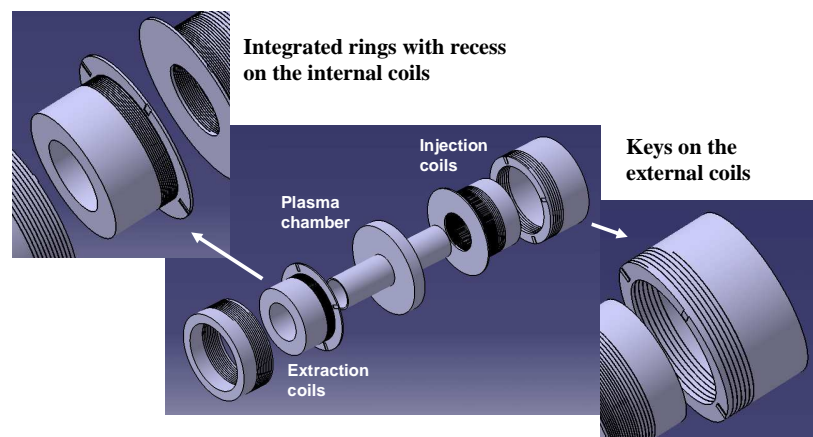


Figure 17. Split view of the coils assembly.

At full current, the maximum hoop stress in the coils is $\sigma \sim 280 \text{ MPa}$, far below the copper alloy limit of elasticity (360 MPa), and the two sets of coils repel each other with a force of 300 kN (30 tons). In case of an extraction coils supply failure (H2+H4), a 50 kN force will arise between H1 and H3 since these two coils have a different magnetic centre. The CAD mechanical design of the magnetic structure, taking in account all these data was performed. Figure 18(a) shows the whole 60 GHz source and Figure 18 (b) represents the intensity and the water courses. The total weight is approximatively 600 kg and dimensions are 620 mm in diameter and 480 mm long.

The mechanical calculus were performed using SAMCEF FIELD, the used norm is CODAP 2005 and the annex GA5 is applied (European directive for pressure equipments 97/23/CE). The structure is designed to support an internal pressure of 43 bars, a repel force of 30 kN and in order to decrease the displacement due to the repel forces.

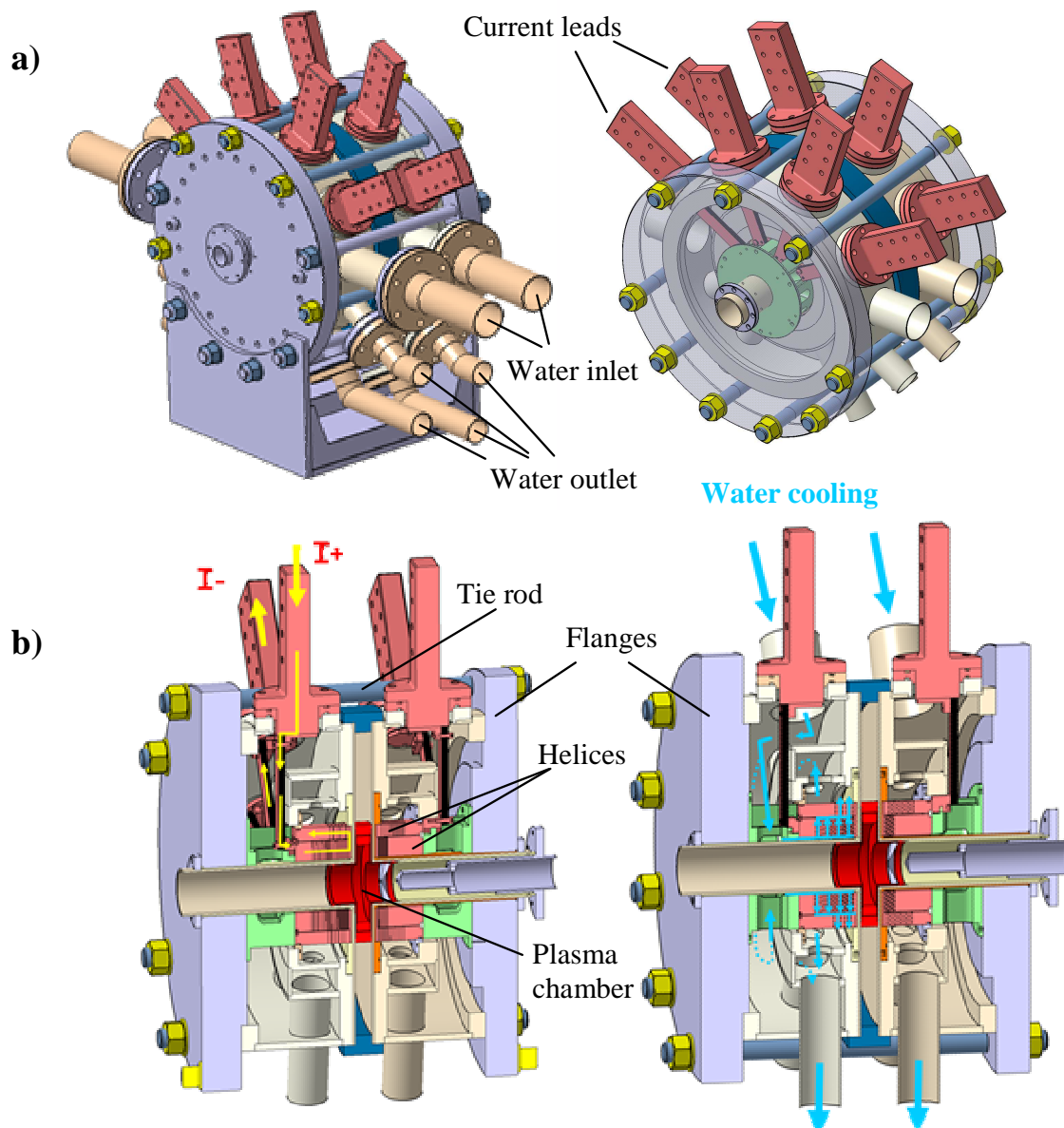


Figure 18. (a) CAD design of the 60 GHz Ion Source, (b) details of the source. Intensity and deionized water courses.

First, all mechanical parts supporting constraints (tubes, ring for support radial forces, flanges etc), were calculated one by one. Then, an axisymmetric model is used as shown in Figure 19 in order to calculate the total displacement and the stress in the whole structure. The total displacement (i.e. the raising distance between the injection and the extraction sets of coils) is of the order of 0.55 mm at full current and the maximum stress is of the order of 170 MPa (except stress concentration).

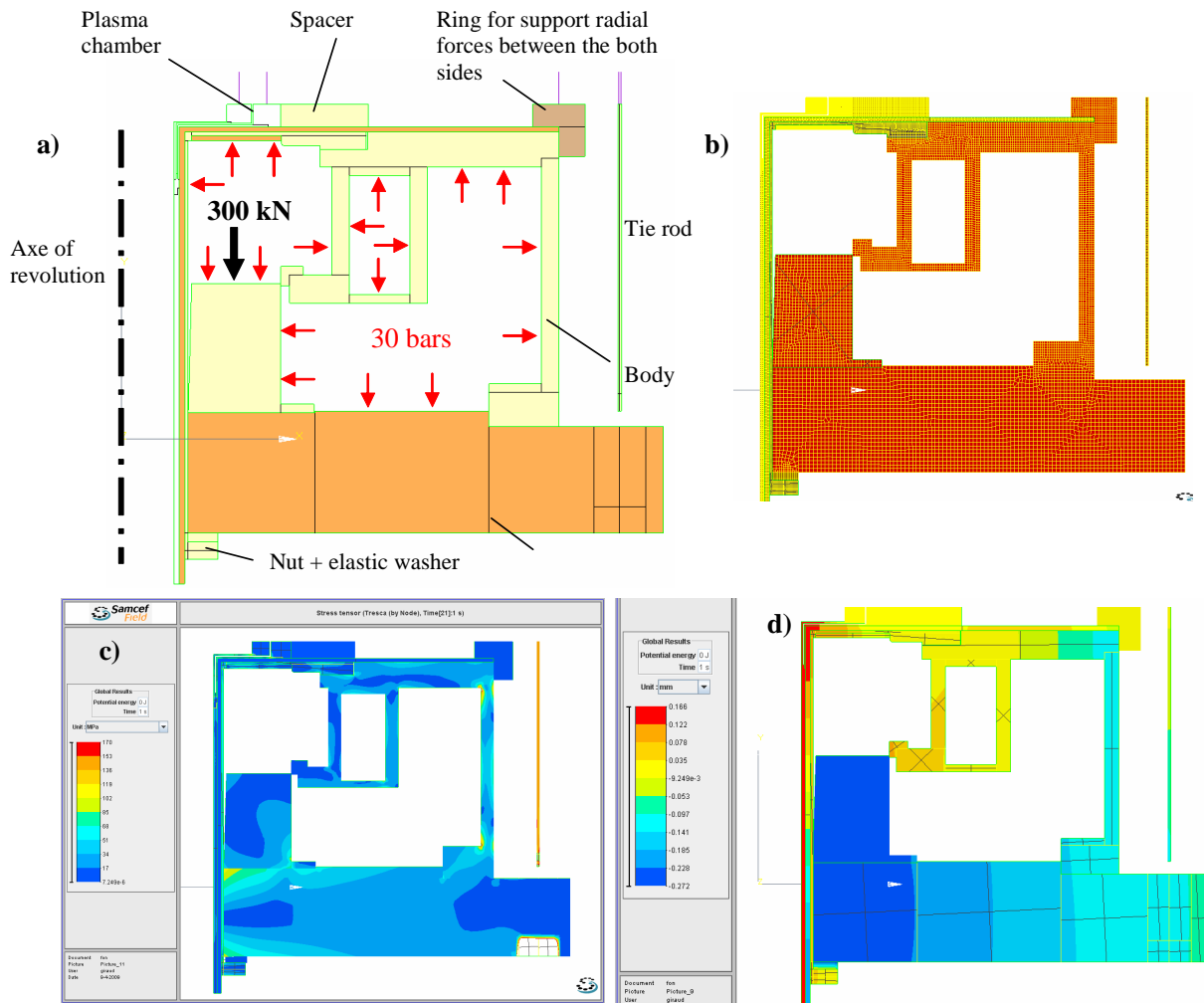


Figure 19. (a) axisymmetric model of one side of the source, some mechanical parts support a 300 kN force and a water pressure of 30 bars; (b) meshing; (c) stress, max stress of 170 MPa in red and (d) displacement, max displacement of -0.27 mm in blue.

3.4 The future test bench

3.4.1 Bending Magnet for the 60 GHz bench

A bending magnet for the future bench (see Figure 20) is available and was developed in collaboration with GANIL and delivered by SIGMAPHI (IN2P3 funding).



Figure 20. Bending Magnet for the 60 GHz bench.

The main characteristics of the bending magnet are the followings:

- 150 mm GAP
- $\Theta=90^\circ$, $\rho=700$ mm
- 350 mm horizontal aperture
- 2.5 Tons
- Mass separation: 100
- $B\rho_{MAX}=0.23$ T.m

3.4.2 The 60 GHz Gyrotron

The 60 GHz gyrotron will be provided by GYCOM (Russia). In 2008, the LPSC received funds from IN2P3 for a total amount of 250 k€ in order to buy the gyrotron which is expected for 2010. The technical specifications are a maximum power available of 100 kW in pulsed mode and an average power of 10 kW in CW mode. It must provide 50 Hz pulses from 15 to 100 ms length. Figure 21 shows a gyrotron frame, a 53 GHz gyrotron and a focusing lens of the Gycom company.

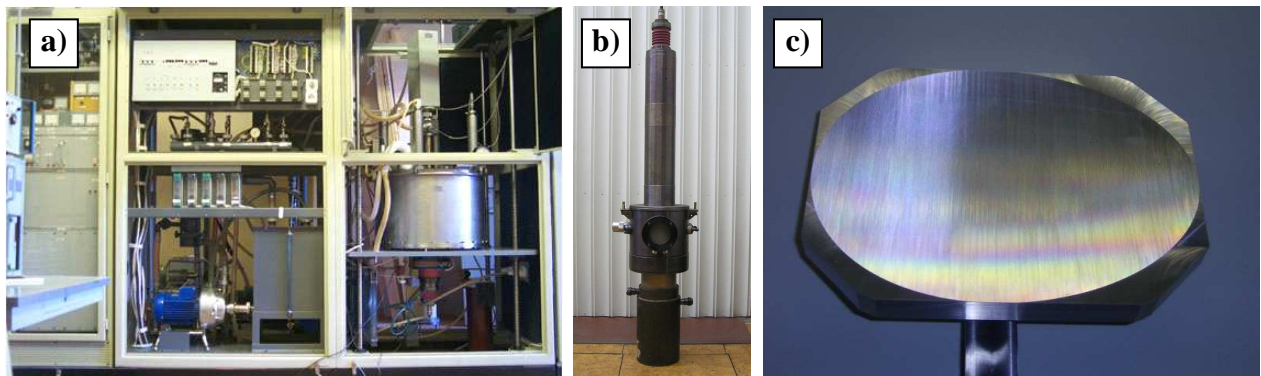
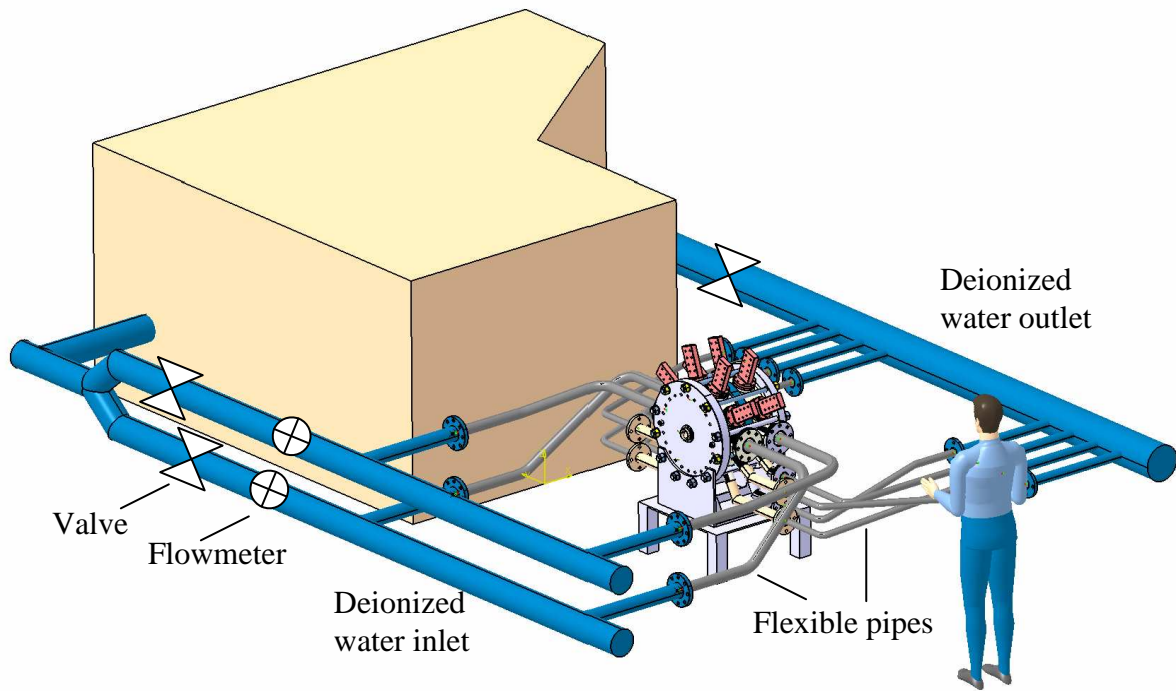


Figure 21. (a) Gycom Gyrotron frame, (b) Gycom Gyrotron 53 GHz 100 kW, (c) IAP Focusing Lens

3.4.3 On-site installation for the half-magnetic field test

Figure 22 represents a schematic view of the temporary on-site setup for the half-magnetic field test. Electrical connections and pipes fittings for cooling are scheduled for the end of august. The flexible power cables are not represented on the figure. For this test at 15000 A, only 20 bars and 22 l/s of water are needed. De-ionized water will be derived in parallel of an existing magnet. The prototype will be series-connected to this magnet in order to dissipate the exceeding power of the current supplies. The average coils temperature should reach only 50 °C while the peak temperature locally reaches 70 °C.



**Figure 22. Installation of the source for the half-magnetic test.
Flexible power cables are not represented.**

4 Planning

This first 60 GHz magnetic structure (helices coils in their tanks, electrical and water cooling environment) should be available in September of 2009 and the half-magnetic field test will follow the same month. The 60 GHz Gyrotron is expected in 2010. First experiments of the prototype at a 28 GHz ECR frequency could be performed at the end of 2009. The first pulsed beam at 60 GHz is expected in 2010.

5 References

- [1] P. Briand, R. Geller and G. Melin, "A newly designed ECR source for the lead injector of CERN," *Nucl. Instrum. Meth. Phys. Res., Sec. A*, Vol. 294(3), p. 673, Sept. 1990.
- [2] P. Sortais, "Pulsed ECR ion source using the afterglow mode," *Rev. Sci. Instrum.*, Vol. 63(4), pp. 2801-2805, Apr. 1992.
- [3] C. Hill and K. Langbein, "Pulsed ECR source in afterglow operation at CERN," *Rev. Sci. Instrum.*, Vol. 67(3), pp. 1328-1330, Mar. 1996.
- [4] P. Sortais, J.L. Bouly, J.-C. Curdy, T. Lamy, P. Sole, T. Thuillier, J.L. Vieux-Rochaz, D. Voulot, "ECRIS development for stable and radioactive pulsed beams," *Rev. Sci. Instrum.*, Vol. 75(5), pp. 1610-1612, May 2004.
- [5] T. Thuillier, J.L. Bouly, J.C. Curdy, E. Froidefond, T. Lamy, C. Peaucelle, P. Sole, P. Sortais, J.L. Vieux-Rochaz, D. Voulot, "High Intensity Ion Beams Prospects for Accelerators with PHOENIX 28 GHz," in *Proc. 8th European Particle Accelerator Conf.*, Paris, 2002, pp. 1744-1746.
- [6] Y. Bykov, G. Denisov, A. Ereemeev, V. Gorbatushkov, V. Kurkin, G. Kalynova, V. Kholoptsev, A. Luchinin, and I. Plotnikov, "28 GHz 10 kW gyrotron system for electron cyclotron resonance ion source," *Rev. Sci. Instrum.*, Vol. 75(5), pp. 1437-1439 May 2004.
- [7] T. Thuillier, T. Lamy, L. Latrasse, I. V. Izotov, A. V. Sidorov, V. A. Skalyga, V. G. Zorin, M. Marie-Jeanne, "Study of pulsed electron cyclotron resonance ion source plasma near breakdown: The Preglow," *Rev. Sci. Instrum.*, Vol. 79(2), 02A314-02A316, Feb. 2008.
- [8] V.E. Semenov, V.A. Skalyga, V.G. Zorin, "Scaling for ECR Sources of Multicharged Ions with Pumping at Frequencies from 10 to 100 GHz," *Rev. Sci. Instrum.*, Vol. 73(2), pp. 635-637, Feb. 2002.

- [9] Izotov I V, Sidorov A V, Skalyga V A, Zorin V G, Lamy T, Latrasse L, Thuillier T 2008 Experimental and theoretical investigation of the Preglow in ECRIS *IEEE Transactions on Plasma Science* **36/4** 1494-501
- [10] E.V. Suvorov and M.D. Tokman, "Theory of microwave breakdown of low-density gas at electron cyclotron resonance in magnetic mirror systems," *Sov. J. Plasma Phys.* Vol. 15, p. 540, 1989, ("K teorii SVCh probuja razrezhennogo gaza v adiabaticheskoy magnitnoj lovushke pri elektronno-tsiklotronnom rezonanse," *Fiz. Plazmy* 15, 934, 1989).
- [11] P. Rub and W. Joss 1996 A new type of radially cooled helices designed for a 25 T magnet *IEEE Transactions on Magnetics* 32 2570 – 3
- [12] O. Chubar, P. Elleaume and J. Chavanne 1998 A three-dimensional magnetostatics computer code for insertion devices *J. Synchrotron Rad.* 5 481 – 4
- [13] C. Trophime, K. Egorov, F. Debray, W. Joss and G. Aubert 2002 Magnet Calculations at the Grenoble High Magnetic Field Laboratory *IEEE Trans. Appl. Superconduct.* 12 1483 – 7
- [14] C. Trophime, S. Krämer and G. Aubert 2006 Magnetic Field Homogeneity Optimization of the Giga-NMR Resistive Insert *IEEE Trans. Appl. Superconduct.* 16 1509 – 12

Related publications and communications

Publications

Izotov I V, Sidorov A V, Skalyga V A, Zorin V G, Lamy T, Latrasse L, Thuillier T 2008 Experimental and theoretical investigation of the Preglow in ECRIS *IEEE Transactions on Plasma Science* **36/4** 1494-501

T. Thuillier, T. Lamy, L. Latrasse, I. V. Izotov, A. V. Sidorov, V. A. Skalyga, V. G. Zorin, M. Marie-Jeanne 2008 Study of pulsed electron cyclotron resonance ion source plasma near breakdown: The Preglow *Rev. Sci. Instrum.* **79(2)** 02A314-6

Thuillier T, Lamy T, Latrasse L, Angot J 2008 First plasma of the A-PHOENIX electron cyclotron resonance ion source, *Rev. Sci. Instrum.* **79(2)** 02A330

T. Thuillier, L. Latrasse, T. Lamy, C. Fourel, J. Giraud, C. Trophime, P. Sala, J. Dumas, F. Debray 2008 High frequency ECR source (60 GHz) in pre-glow mode for bunching of beta-beam isotopes, Proceedings of Science 10th International Workshop on Neutrino Factories, Super beams and Beta beams Valencia, Spain 30 June – 05 July

T. Thuillier, L. Latrasse, T. Lamy, C. Fourel, J. Giraud, C. Trophime, P. Sala, J. Dumas, F. Debray, 60 GHz electron cyclotron resonance ion source for beta-beams Proceedings of the ECRIS08 - 18th International Workshop on ECR Ion Sources (ECRIS08), Proceedings of ECRIS08, Chicago, IL USA (2008) TUCO-A03, 131-5

Communications

Thuillier T, Lamy T, Latrasse L, Izotov I V, Sidorov A V, Skalyga V A, Zorin V G and Marie-Jeanne M, Study of pulsed ECRIS plasma near breakdown: The Preglow, *The 12th International Conference on Ion Sources (ICIS 2007)* Jeju, Korea 26-31 August 2007

Latrasse L, Thuillier T, Lamy T and Marie-Jeanne M, Towards 60 GHz, high intensity pulsed ion beams extracted from 18-28 GHz ECRIS: the Preglow, 2007 *Joint EURISOL EURONS Town Meeting* Helsinki, Finland 17-19 September 2007

L. Latrasse, T. Lamy, T. Thuillier, C. Trophime, F. Debray, J. Dumas, P. Sala, C. Fourel and J. Giraud, 60 GHz Electron Cyclotron Resonance (ECR) Ion Source Prototype: calculus of the magnetic structure and CAD Design, Final EURISOL Town Meeting Pisa, Italy 30 March-1 April 2009